Journal of Controlled Release 268 (2017) 113–119

Contents lists available at ScienceDirect

Journal of Controlled Release

journal homepage: www.elsevier.com/locate/jconrel

Defining optimal permeant characteristics for ultrasound-mediated gastrointestinal delivery

Carl M. Schoellhammer[a,b,c,1], Yiyun Chen[b,d,1], Cody Cleveland[b], Daniel Minahan[b], Taylor Bensel[b], June Y. Park[b], Sarah Saxton[b], Young-Ah Lucy Lee[b], Lucas Booth[b], Robert Langer[a,b,e,f,*], Giovanni Traverso[a,b,g,**]

[a] Department of Chemical Engineering, Massachusetts Institute of Technology, Cambridge, MA 02139, United States
[b] The David H. Koch Institute for Integrative Cancer Research, Massachusetts Institute of Technology, Cambridge, MA 02139, United States
[c] Suono Bio, Inc. 700 Main St., North, Cambridge, MA 02139, United States
[d] Department of Materials, University of Oxford, 16 Parks Road, Oxford OX1 3PH, UK
[e] Institute for Medical Engineering and Science, Massachusetts Institute of Technology, Cambridge, MA 02139, United States
[f] Harvard-MIT Division of Health Science and Technology, Massachusetts Institute of Technology, Cambridge, MA 02139, United States
[g] Division of Gastroenterology, Brigham and Women's Hospital, Harvard Medical School, Boston, MA 02114, United States

ARTICLE INFO

Keywords:
Gastrointestinal drug delivery
Low-frequency ultrasound
Microparticle delivery
Oral delivery
Ultrasound-mediated drug delivery

ABSTRACT

Ultrasound-mediated drug delivery in the gastrointestinal (GI) tract is a bourgeoning area of study. Localized, low-frequency ultrasound has recently been shown to enable significant enhancement in delivery of a broad set of active pharmaceutical ingredients including small molecules, proteins, and nucleic acids without any formulation or encapsulation of the therapeutic. Traditional chemical formulations are typically required to protect, stabilize, and enable the successful delivery of a given therapeutic. The use of ultrasound, however, may make delivery insensitive to the chemical formulation. This might open the door to chemical formulations being developed to address other properties besides the deliverability of a therapeutic. Instead, chemical formulations could potentially be developed to achieve novel pharmacokinetics, without consideration of that particular formulation's ability to penetrate the mucus barrier passively. Here we investigated the effect of permeant size, charge, and the presence of chemical penetration enhancers on delivery to GI tissue using ultrasound. Short ultrasound treatments enabled delivery of large permeants, including microparticles, deep into colonic tissue *ex vivo*. Delivery was relatively independent of size and charge but did depend on conformation, with regular, spherical particles being delivered to a greater extent than long-chain polymers. The subsequent residence time of model permeants in tissue after ultrasound-mediated delivery was found to depend on size, with large microparticles demonstrating negligible clearance from the local tissue 24 h after delivery *ex vivo*. The dependence of clearance time on permeant size was further confirmed *in vivo* in mice using fluorescently labeled 3 kDa and 70 kDa dextran. The use of low-frequency ultrasound in the GI tract represents a novel tool for the delivery of a wide-range of therapeutics independent of formulation, potentially allowing for the tailoring of formulations to impart novel pharmacokinetic profiles once delivered into tissue.

1. Introduction

Gastrointestinal (GI)-based drug delivery is an often preferred means for delivering drugs due to the ease and convenience typically associated with this route of administration [1]. The oral delivery of a broad set of therapeutics remains an area of intense research owing to the challenges presented by the physiology of the GI tract [2]–[4]. Specific challenges around drug delivery to the GI tract include poor drug stability and low solubility of drugs in the gastric environment, low permeability owing to the mucus barrier, and extreme susceptibility to degradation by pH extremes, bacteria and degradative enzymes [5]–[7]. These challenges are amplified further when targeted delivery to a specific location in the GI tract is required, necessitating sophisticated formulation approaches [8]–[10]. Effective oral delivery for the treatment of colonic diseases, like inflammatory bowel disease, for example, not only requires the delivery of an efficacious therapeutic

* Correspondence to: Robert Langer, Department of Chemical Engineering, Massachusetts Institute of Technology, Cambridge, MA 02139, United States.
** Correspondence to: Giovanni Traverso, The David H. Koch Institute for Integrative Cancer Research, Massachusetts Institute of Technology, Cambridge, MA 02139, United States.
E-mail addresses: rlanger@mit.edu (R. Langer), gi_lab@mailworks.org (G. Traverso).
[1] These authors contributed equally to this work

http://dx.doi.org/10.1016/j.jconrel.2017.10.023
Received 29 March 2017; Received in revised form 1 October 2017; Accepted 13 October 2017
Available online 16 October 2017

to the affected site but also protection of the molecule from the harsh, proximal GI environment. Moreover, targeting to the site of disease can be a complex formulation challenge, utilizing pH-responsive nanoparticles [11] or surface modifications to enable high selectivity [12].

These hurdles largely stem from the need for the formulation to play two roles: i) encapsulation and protection of the therapeutic from the gastric environment, and ii) high target-specificity to minimize off-target effects [8,13]. These two roles often require disparate formulation strategies, leading to therapeutics with low bioavailability and inadequate target specificity [14,15]. The ability to decouple these two requirements such that the formulation no longer has to satisfy both requirements may help expedite translation of successful therapeutics to the clinic [16]. Physical enhancers are one such method that may enable formulation-independent delivery of material and interest in their use in the GI tract has recently increased [17,18]. Ultrasound, one type of physical enhancer, has recently begun to be investigated in the GI tract with potentially broad utility, allowing the successful delivery of small molecules, biologics, and nucleic acids in an enema format [17,19].

Ultrasound is a sound wave characterized as having a frequency above the audible range of humans ($>$ 20 kHz) [20]. Ultrasound has seen broad clinical use for a myriad of applications, including imaging, lithotripsy, and lysis of fat during liposuction [21]. With respect to drug delivery, ultrasound has been investigated for decades for transdermal drug delivery [22]. The enhancement in drug uptake using ultrasound relies on a phenomenon known as acoustic cavitation [23]. When an ultrasound wave is propagating through a fluid, the oscillating pressure field spontaneously nucleates bubbles in the solution [20]. Using low-frequency ultrasound, ($\leq$ 100 kHz) these bubbles grow through rectified diffusion, and eventually become unstable [24]. They then implode, causing a microjet [25]. These microjets can physically propel drug into tissue and reversibly permeabilize tissue to allow enhanced drug uptake [17,26].

Clinically, ultrasound might lend itself to drug delivery applications in the GI tract, in addition to the skin. One such embodiment of the technology in the GI tract could be the administration of medicated enemas for targeted delivery to the rectum in the setting of diseases such as ulcerative colitis [27]. More broadly, ultrasound is also readily miniaturizable, which may enable fully ingestible capsules for the oral delivery of therapeutics currently limited to injection [28,29]. Given the potentially broad use ultrasound might have for drug delivery and the fact that its previously been shown to enable formulation-independent delivery of proteins and nucleic acids [17,19], this study sought to identify and characterize permeant properties that can modulate delivery and retention in GI tissue.

2. Materials and methods

2.1. Chemicals

Phosphate buffered saline (PBS), dextran labeled with Texas red (3 kDa and 70 kDa), dextran labeled with tetramethylrhodamine (2000 kDa), and carboxylate-modified and amine-modified polystyrene microspheres were obtained from Thermo Fisher Scientific (Waltham, MA). Sodium hydroxide was obtained from Amresco (Solon, OH). Sodium lauryl sulfate (SLS) and formalin were obtained from Sigma-Aldrich (Saint Louise, MO). All chemicals were used as received.

2.2. Tissue procurement

This research was approved by the Massachusetts Institute of Technology (MIT) Committee on Animal Care. Fresh GI tissue from Yorkshire pigs was procured within an hour of sacrifice. The tissue was washed thoroughly using PBS and excess fat dissected away. The tissue was sectioned into pieces approximately 2 cm × 2 cm for subsequent mounting in Franz diffusion cells with an exposed area for delivery of 15-mm (PermeGear, Hellertown, PA). First the receiver chamber was filled with PBS and the tissue placed on top of the receiver chamber with the muscularis layer in contact with the receiver chamber. A donor chamber was then placed on top of the tissue and the setup clamped together. PBS was added to the donor chamber to keep the tissue hydrated before treatment. Care was taken to ensure there were no air bubbles in the receiver chamber. Experiments were conducted at room temperature.

2.3. Ultrasound treatment

Ultrasound was generated with a 20 kHz, VCX500 probe from Sonics & Materials (Newtown, CT). Ultrasound was applied with the transducer positioned 3 mm above the tissue surface at an intensity of 5 W/cm^2 calibrated by calorimetry [30]. A 50% duty cycle was utilized to reduce thermal effects [31]. Immediately before treatment, the PBS was removed from the donor chamber and the coupling fluid containing the permeant of interest was added. Fluorescently labeled probes were used as the model permeants and used at a concentration of 0.2 mg/mL unless otherwise stated.

2.4. Delivery quantification in tissue

Permeant content in the tissue after delivery was quantified using an *In Vivo* Imaging System (IVIS) Fluorescent Imager (PerkinElmer, Waltham, MA). Immediately after ultrasound treatment, the donor chamber solution was discarded and the tissue washed. Tissue samples were then imaged with the IVIS Fluorescent Imager. Unless otherwise noted, imaging was performed using a binning factor of 8, f-stop of 8, and a field of view of 21.6 cm. Exposure time was varied to ensure a total photon count of $\geq$ 6000, per the manufacturer's guidelines.

2.5. Tissue clearance tests

Permeant clearance from tissue samples was also investigated *ex vivo*. Tissue samples were treated in Franz diffusion cells as described. After treatment, the treated tissue samples were thoroughly washed and placed in individual 500 mL beakers filled with 300 mL PBS to mimic an infinite-sink condition. All beakers were stirred on a magnetic stir plate at 400 rpm. 24 h after treatment, tissue samples were removed from the beakers, thoroughly washed, and imaged using an IVIS Fluorescent Imager.

2.6. Scanning electron microscopy (SEM)

In order to image microparticles within tissue after delivery, samples were imaged by scanning electron microscopy using a JEOL JSM-5000 Scanning Electron Microscope and Environmental Scanning Electron Microscope. Samples were prepared for imaging by dehydration in 200 proof ethanol at serial concentrations of 50%, 75%, 90%, 95%, and 100% ethanol. Dehydration in each concentration lasted 20 min. Ethanol-dehydrated samples were finally dried using a critical point drying instrument. Dried samples were mounted on aluminum stages using carbon black stickers and coated with gold nanoparticles by spattering. Samples were imaged using an acceleration voltage of 5 kV, working distance of 20 mm and a spot size of 20 at various magnifications.

2.7. Confocal microscopy

Fluorescently labeled permeants were also imaged for their distribution within tissue by confocal microscopy. After ultrasound treatment, the tissue was thoroughly washed and removed from the Franz diffusion cells. Tissue was fixed with 10% formalin overnight. After fixation, tissue samples were stained with 4′,6-diamidino-2-phenylindole, dihydrochloride (DAPI) nuclear stain for 30 min.

All images were acquired using an Olympus FV1000 Multiphoton Laser Scanning Microscope with a step depth of 5 μm. Step counts started at the surface (step 0) and imaged 26 steps in the z-direction (125 μm depth). Three channels were imaged, including the fluorescent label, the second harmonic to visualize collagen networks and tissue structure, and DAPI.

2.8. In Vivo mouse clearance studies

All animal experiments were performed in accordance with protocols approved by the Committee on Animal Care at MIT. Female, C57BL/6 mice 15 weeks old were used for this study. Animals were anesthetized using isoflurane during the treatment. A custom-made 40 kHz ultrasound probe was used to administer ultrasound locally in the colon (Sonics and Materials, Inc., Newtown, CT) [17]. The intensity of treatment was calibrated to 4.0 W by calorimetry. Treatment consisted of a 0.5 s burst of ultrasound.

3 kDa and 70 kDa Texas red-labeled dextrans were used as model permeants to maintain a constant permeant chemistry while isolating the effect of permeant size. A 0.5 mL enema of dextran at a concentration of 0.33 mg/mL was instilled into the colon. The ultrasound probe was immediately inserted into the colon and sonication took place for approximately 0.5 s. After sonication, the ultrasound probe was removed with the animal still sedated by isoflurane. The dextran solution was allowed to sit in the colon for 2 min. After that time, the colon was thoroughly lavaged with PBS to remove any residual dextran that did not penetrate the tissue. Groups of animals were euthanized immediately after, or 30 min after the excess dextran was washed out of the colon. After sacrifice, the animals' colons were dissected out. Fluorescent intensity was quantified by imaging the colons using an IVIS Fluorescent Imaging System (Perkin-Elmer, Waltham, MA) using the same procedure described above.

2.9. Statistical analysis

Statistical analysis was performed using one-way analysis-of-variance (ANOVA) tests with multiple comparisons unless otherwise stated. Statistical significance was defined as $P < 0.05$. All statistical calculations were performed in MatLab R2015a.

3. Results and discussion

3.1. Effect of material size on delivery

The impact of permeant size on its ability to be delivered using ultrasound was investigated first. It was hypothesized that larger permeants and particles would be delivered to a lesser extent because of increased steric hindrance. Latex beads with diameters spanning two orders of magnitude and dextran polymers were utilized to examine the effect of both rigid defined shapes (latex particles) and free polymer chains (dextrans). At the same time, the effect of size alone may be isolated by utilizing the same chemistries for both conformational types. Fluorescent intensity was correlated to mass of the permeant using a calibration curve. Delivery of various permeants into tissue is shown in Fig. 1 using the permeants at a concentration of 0.2 mg/mL in the donor chamber.

Despite the order-of-magnitude difference in bead diameters tested, consistent delivery was achieved using ultrasound, showing no significant dependence on permeant size. The same result was observed using dextran ranging in molecular mass from 70 kDa to 2000 kDa. Despite testing two different conformations of materials, namely rigid, spherical particles and free polymer chains, consistent delivery was observed over a wide range of sizes. Interestingly, the number of latex beads delivered into tissue was an order of magnitude greater than the amount of dextran delivered, despite the smaller size of the dextran permeants tested. This is thought to be a result of the ultrasound acting on the permeant, actively propelling it into the tissue. The importance of the effect of ultrasound acting on the permeant as opposed to the tissue has previously been noted in experiments investigating delivery using both pre-treatment of tissue with ultrasound as well as simultaneous permeant-ultrasound exposure, with the latter showing significantly greater delivery [17].

With regard to the effect of ultrasound on the tissue, SEM imaging was performed on tissue treated with ultrasound and compared to tissue not treated with ultrasound. Representative images are shown in Fig. 2. In tissue not treated with ultrasound (Fig. 2A), crypts were not visible and were obscured by the thick mucus layer that covers GI epithelial surfaces. However, in tissue treated with ultrasound (Fig. 2B), the crypts were clearly visible and were distributed evenly as expected.

Therefore, it seems that ultrasound acts to dissipate the mucus layer to facilitate enhanced delivery, as opposed to altering the epithelial structure. This is in agreement with other published studies, which noted negligible histological disruption to the surface colonic epithelium resulting from ultrasound treatment [17]. Because mucus is continuously secreted, it is hypothesized that this layer would regenerate after treatment [32]–[34]. Indeed, previous reports on chronic administration of ultrasound in the rectum have shown no deleterious effects, even in the setting of chemically-induced inflammation [17,19]. The subsequent distribution of latex beads over the tissue as a result of delivery was also imaged (Fig. 2C). Treatment enabled relatively uniform distribution of the latex beads across the epithelial surface, with no clear pattern in clustering or location of the beads after delivery.

The penetration of latex beads within the tissue was also investigated using confocal microscopy. Confocal imaging was performed on porcine colonic tissue following delivery of fluorescently labeled 0.5 μm diameter carboxylate-modified latex beads and staining with DAPI. Discrete levels within the tissue are shown in Fig. 3. Penetration into the tissue was also relatively uniform, although some clustering was observed. Interestingly, fluorescent signal was observed at depths of up to 125 μm into the tissue from the ultrasound exposed luminal surface, demonstrating significant penetration of permeants as a result of a short ultrasound treatment. The fact that relatively large particles can be delivered deep within the tissue using ultrasound might enable the development of depot systems for the extended release of therapeutics locally in the colon.

3.2. Effect of surface charge on delivery

Next, the effect of surface charge was investigated. Given the anionic nature of mucus, charge is an important parameter that is utilized in GI-based drug formulations to modulate retention and delivery [35]. To investigate the effect of material charge on delivery, latex beads with carboxyl or amine surface modifications were utilized to impart charge on the particle. The delivery of 0.2 μm diameter beads with either amine (+0.3 a-equivalents per particle) or carboxyl (−0.3 a-equivalents per particle) surface modifications is shown in Fig. 4. Surface charge was found to not significantly affect the amount of material delivered into the tissue using ultrasound. This was surprising given the mucus layer is negatively charged and the epithelium is positively charged [5]. This, again, seems to support the hypothesis that the predominant mechanism of ultrasound-mediated GI delivery is ultrasound acting on the permeant, as opposed to ultrasound permeabilizing the tissue directly. This would have tremendous benefit when considering the safety of this technology. If delivery is independent of charge of the material, then charge may be a parameter that could be tuned to achieve subsequent retention or preferential clearance from the tissue after ultrasound-mediated delivery. This would need to be investigated further.

3.3. Effect of treatment time on delivery

Given the relative insensitivity of delivery to permeant size or

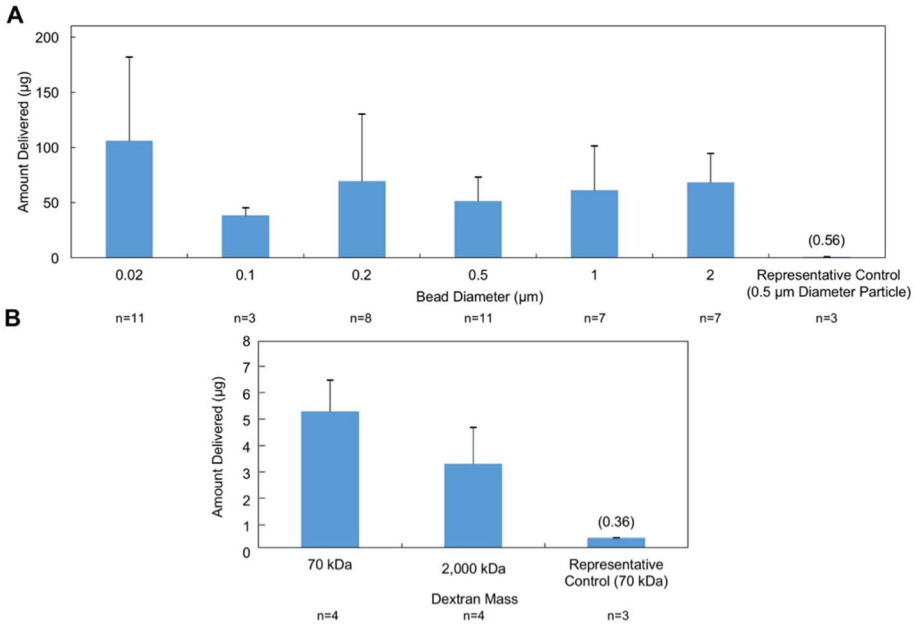

Fig. 1. Ultrasound-mediated delivery of fluorescently-labeled latex beads (A) and dextran polymers (B) of different sizes into porcine colonic tissue *ex vivo* compared to delivery without ultrasound (control). Data represent averages + 1SD. Ultrasound-mediated delivery was significantly greater than delivery without ultrasound. No significant difference was found between different permeant sizes delivered using ultrasound (determined by one-way ANOVA with multiple comparisons). Sample size indicates biological repeats.

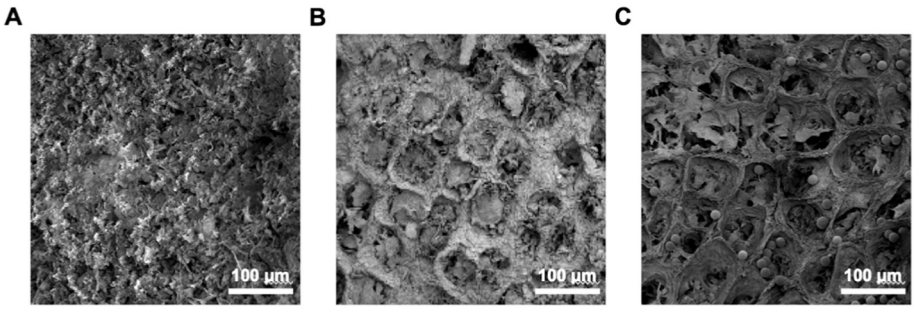

Fig. 2. SEM micrographs of porcine colonic tissue not treated with ultrasound (A) and after treatment with ultrasound (B). (C) Porcine colonic tissue after simultaneous treatment with ultrasound and 15 μm diameter latex beads.

charge, the ultrasound treatment time utilized was varied to investigate its effect on delivery. Previous studies have utilized treatment times of 60 s exclusively [17]. Therefore, a range of treatment times was investigated here to understand in greater detail how materials interact with ultrasound. It was hypothesized that delivery would directly correlate with ultrasound treatment time.

Treatment times between 10 and 150 s of ultrasound (20–300 s total permeant contact time utilizing a 50% duty cycle) were tested for three different permeants having a range of molecular masses and conformations (Fig. 5).

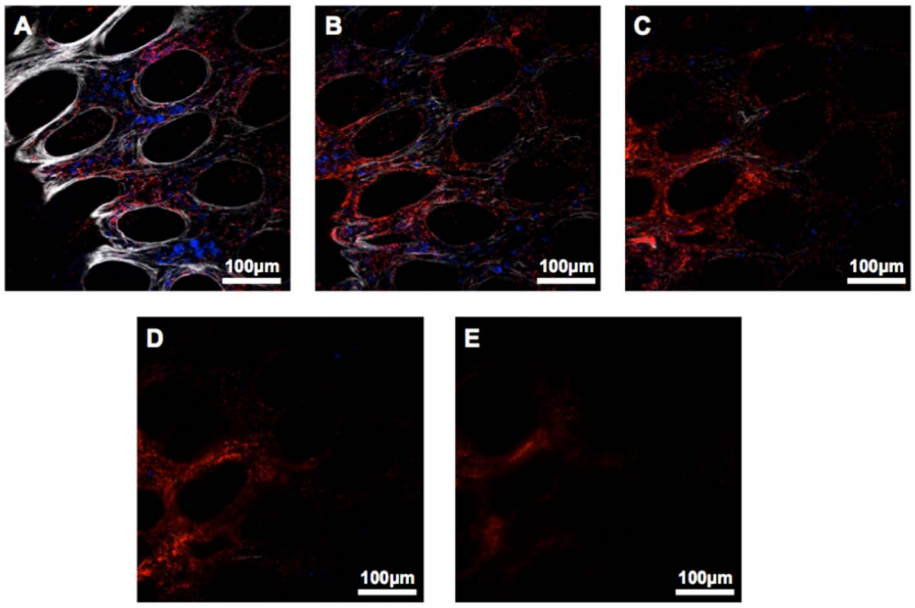

Fig. 3. Z-stack confocal images of porcine colonic tissue after delivery of 0.5 μm diameter carboxylate-modified latex beads and staining with DAPI. Depths of 25 μm (A), 50 μm (B), 75 μm (C), 100 μm (D), and 125 μm (E) into tissue are shown. The latex particles (red), DAPI nuclear stain (blue) and second harmonics representing the tissue architecture (white) are shown. (For interpretation of the references to colour in this figure legend, the reader is referred to the web version of this article.)

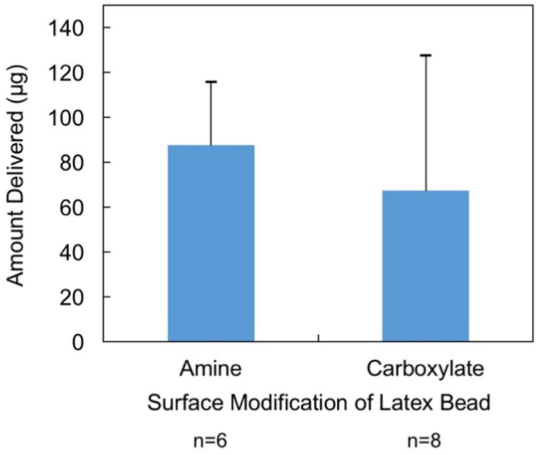

Fig. 4. Delivery of 0.2 μm diameter fluorescently labeled latex beads with different surface modifications into porcine colonic tissue *ex vivo*. Amine-modified beads are cationic and carboxylate-modified beads are anionic. Data represent averages + 1SD. $P > 0.1$ by Student's two-tailed *t*-test. Sample size indicates biological repeats.

Generally, the amount of permeant delivered into tissue increased with increasing ultrasound treatment time, as expected. The delivery of 70 kDa dextran correlated almost linearly with ultrasound treatment time. Interestingly, the delivery of 2000 kDa dextran appeared to plateau with increasing ultrasound treatment time, reaching a maximum in delivery at a treatment time of 90 s. This result suggests that no further penetration of 2000 kDa into tissue occurs with further ultrasound exposure. No such plateau was observed in the delivery of 70 kDa dextran or 0.5 μm diameter latex beads. If this plateau were simply a result of permeant size, then it would be expected that delivery of 0.5 μm diameter latex beads would also show a similar plateau. However, that was not the case (Fig. 5C). Indeed, the delivery of 0.5 μm diameter latex beads increased with increasing ultrasound treatment time. Together, these findings suggest the plateau in delivery of 2000 kDa dextran may be due to another material property beyond simply the permeant's size or mass. For example, the permeant conformation, in addition to overall size, may also play an important part in determining its deliverability and may explain why a long-chain polymer like 2000 kDa dextran demonstrated a plateau in delivery. Additional investigations would be needed to fully elucidate the effect of permeant conformation on its subsequent deliverability with ultrasound.

3.4. Effect of the simultaneous use of chemical penetration enhancers

In addition to treatment time, the use of chemical penetration enhancers (CPEs) was investigated because they have previously been shown to act synergistically with ultrasound in the context of transdermal drug delivery [25]. However, the potential synergy of ultrasound and CPEs has not previously been investigated in the GI tract. SLS at a concentration of 1 wt% was chosen because it has been commonly employed in transdermal and oral drug delivery studies [3,36]. SLS was hypothesized to further enhance delivery based on achieving an increased level of tissue permeabilization. The resulting delivery of model permeants with and without SLS is shown in Fig. 6A. It can be seen that the delivery of 2000 kDa dextran and 0.5 μm diameter carboxylate-modified latex beads was significantly reduced by the addition of SLS to the coupling solution. The average amount of 70 kDa dextran was also reduced using SLS, however this result was not statistically significant. Multiple issues might be attributed to this result. First, there could be static repulsion effects owing to the fact that the 2000 kDa dextran, 0.5 μm diameter carboxylate-modified latex beads, and the SLS are all negatively charged, whereas the 70 kDa dextran is zwitterionic. Another possible explanation could be the fact that SLS reduces the surface tension of the coupling solution, leading to reduced energetics of bubble collapse during transient cavitation [20]. Given the findings presented above on the negligible role surface charge plays on delivery, it is thought that delivery is reduced upon the application of SLS because of reduced bubble collapse energetics. This would indeed result in heavier permeants being delivered less, which is what was observed in Fig. 6A.

3.5. Permeant clearance tests

In addition to delivery into tissue, the subsequent clearance of the drug material can play an important role in the overall therapeutic effect. Therefore, the clearance time of model permeants from tissue was investigated after ultrasound-mediated delivery into tissue. While SLS had no effect on the immediate delivery of 70 kDa dextran, perhaps an effect would be seen at longer time scales, which would allow more time for SLS to act on the tissue to fluidize and subsequently permeabilize the barrier. As a result of increased permeability, it was hypothesized that the addition of SLS would increase the rate of clearance of materials from tissue. The results are shown in Fig. 6B.

With the exception of 2000 kDa dextran, the addition of SLS in the donor chamber during ultrasonic treatment resulted in significantly less permeant still present in the tissue 24 h later. The addition of SLS had no effect on the clearance of 2000 kDa dextran. This result could be an artifact due to the resolution attainable using fluorescent probes and the inherent noise. Given the significant reduction in the delivery of 2000 kDa dextran observed using SLS (Fig. 6A(ii)), further reductions in signal due to clearance of the 2000 kDa dextran after 24 h could make detecting the fluorescent signal above background noise, difficult. This could also explain the larger standard deviation observed in the 24-h clearance results using SLS. However, the exact cause of this observation is still unclear and more experiments would be needed in order to better understand the impact.

When SLS was not used during ultrasonic delivery, clearance was reduced, resulting in more permeant remaining in the tissue 24 h after delivery. It can be seen that for both masses of dextran, approximately 80% of the initial amount of material had cleared from the tissue after 24 h using SLS during delivery. In contrast, the 0.5 μm diameter carboxylate-modified latex beads showed significantly less clearance (Fig. 6B(vi)) when SLS was used during delivery. Even more striking, when SLS was not used, there was found to be no clearance of latex beads from the tissue 24 h after delivery. This lack of clearance from the tissue is thought to be a result of the relatively large size of these particles, which would hinder their diffusion through the tissue after delivery with ultrasound. Based on this result, material size is likely to directly correlate with the residence time of the material in GI tissue and may offer an important variable for tuning novel pharmacokinetic

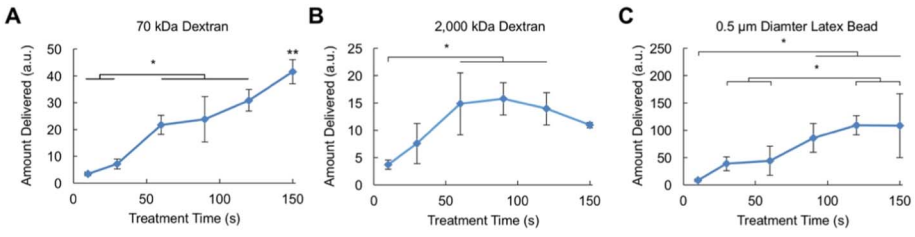

Fig. 5. Delivery of fluorescently labeled permeants into porcine colonic tissue *ex vivo vs.* ultrasound treatment time for 70 kDa (A), 2000 kDa (B) dextran, and 0.5 μm diameter carboxylate-modified latex beads (C). Data represent averages ± 1SD. * indicates $P < 0.05$ by one-way ANOVA with multiple comparisons. ** represents $P < 0.05$ compared to all other treatment times. Each condition represents 3–12 biological repeats.

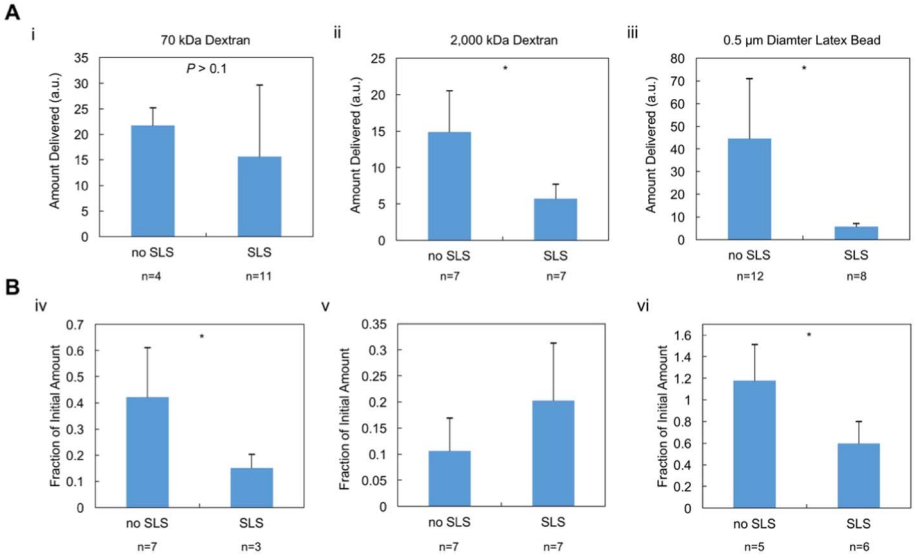

Fig. 6. (A) Delivery of fluorescently labeled permeants into porcine colonic tissue *ex vivo* with and without SLS for 70 kDa dextran (i), 2000 kDa dextran (ii), and 0.5 μm diameter carboxylate-modified latex beads (iii). (B) Fraction of the initial amount of material delivered into tissue after 24-h clearance studies in the presence of SLS. The amount of 70 kDa dextran (iv), 2000 kDa dextran (v), and 0.5 μm diameter carboxylate-modified latex beads (vi) are shown after 24 h normalized to their initial values. Data represent averages + 1SD. ** indicates $P < 0.05$ by two-tailed Student's *t*-tests. Sample size indicates biological repeats.

profiles of therapeutics administered using ultrasound. This extended residence time again supports the idea that depot systems could be created to allow for extended or controlled release of drug locally in GI tissue.

3.6. In Vivo testing of clearance rate

Given the observed impact of molecular weight on subsequent clearance of permeants from the local tissue, this effect was investigated further *in vivo* in mice using 3 and 70 kDa dextran so as to isolate the effect of molecular size only. The two permeants were administered rectally followed by sonication using a custom-made ultrasound probe (Fig. 7A) [17,19]. The relative amount of each permeant still present in the colonic tissue *in vivo* 30 min after delivery is shown in Fig. 7B.

From Fig. 7B, it can be seen that after 30 min, statistically more 3 kDa dextran had been cleared from the colon than 70 kDa dextran. Indeed, in 30 min, only 34% of the 70 kDa dextran had been cleared from the colon, as opposed to 86% of the 3 kDa dextran. Because the only difference between the two permeants is length of the polymer chain, the decreased rate of clearance observed *in vivo* for 70 kDa dextran may be attributed to its size. Based on the Stokes Radius, 70 kDa dextran has a radius approximately 2.5 × larger than the radius of 3 kDa dextran [37]. This simple increase in molecular size has a powerful impact on subsequent clearance and serves as a proof-of-concept for tuning of the size of hypothetical drug formulations to modulate residence times in the tissue to achieve extended release.

4. Conclusions

Ultrasound-mediated gastrointestinal delivery has the capacity to rapidly deliver a wide-range of permeants with little sensitivity to the permeant itself. Short, 1-min treatments significantly enhanced permeation and delivery of materials into epithelial tissue to depths beyond 100 μm *ex vivo*. This was observed irrespective of the surface charge of the permeant, which was surprising given the net negative charge of mucus. Ultrasound treatments appeared to remove the mucus layer, revealing the crypts, which could explain why anionic microparticles were delivered to the same extent as cationic ones. The morphology of the permeant impacted delivery, with homogenous, spherical latex beads being delivered to a greater extent than long-chain polymers (dextran). Once delivered into tissue, permeant size was discovered to play an important role in the overall residence time in the tissue. Larger permeants are retained longer in tissue, owing to their reduced diffusion through tissue as a result of their size. This result was also confirmed *in vivo* in mice with 70 kDa dextran being cleared more slowly from the colon than 3 kDa dextran. This technology could be used clinically for the administration of medicated enemas, enabling the localized delivery of biologics to treat diseases such as inflammatory bowel disease. More broadly, these studies will help inform further development and miniaturization of ultrasound technology to enable fully-ingestible systems for the oral delivery of complex molecules.

Funding

This research was funded by the National Institutes of Health

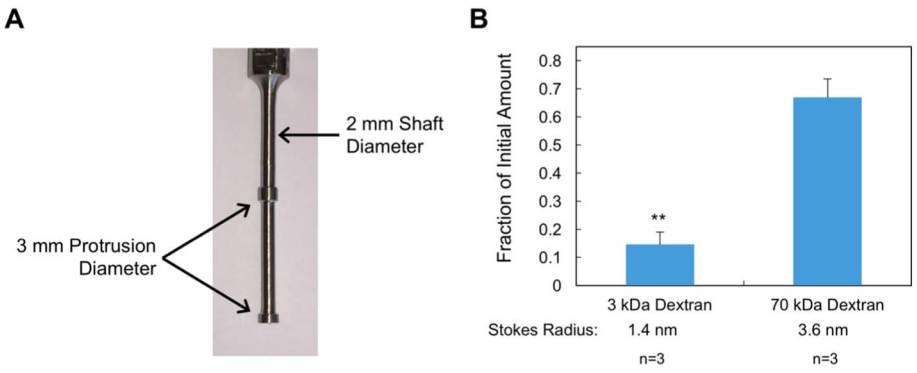

Fig. 7. (A) A miniaturized 40 kHz ultrasound probe for local administration in mice. The protrusions initiate radial ultrasound activity. (B) Fraction of the initial amount of material delivered into mouse colonic tissue *in vivo* 30 min after administration. Data represents averages + 1SD. ** Represents $P < 0.05$ compared to the amount of each permeant delivered into tissue immediately after treatment by a two-tailed Student's *t*-test. Sample size indicates biological repeats.

(Grant# EB-000244), and Max Planck Research Award (to R.L.), Award Ltr Dtd. 2/11/08, Alexander von Humboldt-Stiftung Foundation. G.T. was supported in part by the Division of Gastroenterology, Brigham and Women's Hospital. C.M.S. was supported in part by a Koch Institute Quinquennial Cancer Research Fellowship.

Competing interests

C.M.S., R.L. and G.T. are co-inventors on multiple patents describing the application of ultrasound for delivery in the GI tract. C.M.S. is an employee of Suono Bio, Inc. a biotechnology focused on the development of ultrasound-based systems for drug delivery. C.M.S., R.L. and G.T. have a financial interest in Suono Bio, Inc.

Acknowledgements

We thank J. Wyckoff of the Microscopy Core Facility in the Swanson Biotechnology Center for imaging samples and the Hope Babette Tang (1983) Histology Core Facility.

References

[1] L.M. Ensign, R. Cone, J. Hanes, Oral drug delivery with polymeric nanoparticles: the gastrointestinal mucus barriers, Adv. Drug Deliv. Rev. 64 (6) (2012) 557–570.
[2] S. Mitragotri, P.A. Burke, R. Langer, Overcoming the challenges in administering biopharmaceuticals: formulation and delivery strategies, Nat. Rev. Drug Discov. 13 (9) (Aug. 2014) 655–672.
[3] K. Whitehead, N. Karr, S. Mitragotri, Safe and effective permeation enhancers for oral drug delivery, Pharm. Res. 25 (8) (2008) 1782–1788.
[4] Y.-A.L. Lee, S. Zhang, J. Lin, R. Langer, G. Traverso, A Janus mucoadhesive and omniphobic device for gastrointestinal retention, Adv. Healthcare Mater. 5 (10) (May 2016) 1141–1146.
[5] R.A. Cone, Barrier properties of mucus, Adv. Drug Deliv. Rev. 61 (2) (Feb. 2009) 75–85.
[7] M. Goldberg, I. Gomez-Orellana, Challenges for the oral delivery of macromolecules, Nat. Rev. Drug Discov. 2 (4) (Apr. 2003) 289–295.
[8] D.S. Wilson, G. Dalmasso, L. Wang, S.V. Sitaraman, D. Merlin, N. Murthy, Orally delivered thioketal nanoparticles loaded with TNF-α–siRNA target inflammation and inhibit gene expression in the intestines, Nat. Mater. 9 (11) (Oct. 2010) 923–928.
[10] T. Gajanayake, R. Olariu, F.M. Leclere, A. Dhayani, Z. Yang, A.K. Bongoni, Y. Banz, M.A. Constantinescu, J.M. Karp, P.K. Vemula, R. Rieben, E. Vogelin, A single localized dose of enzyme-responsive hydrogel improves long-term survival of a vascularized composite allograft, Sci. Transl. Med. 6 (249) (Aug. 2014) 249ra110.
[11] K. Sonaje, K.-J. Lin, J.-J. Wang, F.-L. Mi, C.-T. Chen, J.-H. Juang, H.-W. Sung, Self-assembled pH-sensitive nanoparticles: a platform for oral delivery of protein drugs, Adv. Funct. Mater. 20 (21) (Oct. 2010) 3695–3700.
[12] Y. Jin, Y. Song, X. Zhu, D. Zhou, C. Chen, Z. Zhang, Y. Huang, Goblet cell-targeting nanoparticles for oral insulin delivery and the influence of mucus on insulin transport, Biomaterials 33 (5) (Feb. 2012) 1573–1582.
[13] A. Frede, B. Neuhaus, R. Klopfleisch, C. Walker, J. Buer, W. Müller, M. Epple, A.M. Westendorf, Colonic gene silencing using siRNA-loaded calcium phosphate/PLGA nanoparticles ameliorates intestinal inflammation in vivo, J. Control. Release 222 (Jan. 2016) 86–96.
[14] E.M. Pridgen, F. Alexis, T.T. Kuo, E. Levy-Nissenbaum, R. Karnik, R.S. Blumberg, R. Langer, O.C. Farokhzad, Transepithelial transport of fc-targeted nanoparticles by the neonatal fc receptor for oral delivery, Sci. Transl. Med. 5 (213) (Nov. 2013) 213ra167.
[15] A. Banerjee, J. Qi, R. Gogoi, J. Wong, S. Mitragotri, Role of nanoparticle size, shape and surface chemistry in oral drug delivery, J. Control. Release 238 (Sep. 2016) 176–185.
[16] C.M. Schoellhammer, G. Traverso, Low-frequency ultrasound for drug delivery in the gastrointestinal tract, Expert Opin. Drug Deliv. 13 (8) (Aug. 2016) 1045–1048.
[17] C.M. Schoellhammer, A. Schroeder, R. Maa, G.Y. Lauwers, A. Swiston, M. Zervas, R. Barman, A.M. DiCiccio, W.R. Brugge, D.G. Anderson, D. Blankschtein, R. Langer, G. Traverso, Ultrasound-mediated gastrointestinal drug delivery, Sci. Transl. Med. 7 (310) (Oct. 2015) 310ra168.
[18] C.M. Schoellhammer, R. Langer, G. Traverso, Of microneedles and ultrasound: physical modes of gastrointestinal macromolecule delivery, Tissue Barriers 4 (2) (Apr. 2016) e1150235.
[19] C.M. Schoellhammer, G.Y. Lauwers, J.A. Goettel, M.A. Oberli, C. Cleveland, J.Y. Park, D. Minahan, Y. Chen, D.G. Anderson, A. Jaklenec, S.B. Snapper, R. Langer, G. Traverso, Ultrasound-mediated delivery of RNA to colonic mucosa of live mice, Gastroenterology 152 (5) (Jan. 2017) 1151–1160.
[20] B.E. Polat, D. Hart, R. Langer, D. Blankschtein, Ultrasound-mediated transdermal drug delivery: mechanisms, scope, and emerging trends, J. Control. Release 152 (3) (Jun. 2011) 330–348.
[21] D. Miller, N. Smith, M. Bailey, G. Czarnota, K. Hynynen, I. Makin, American Institute of Ultrasound in Medicine Bioeffects Committee, Overview of therapeutic ultrasound applications and safety considerations, J. Ultrasound Med. 31 (4) (Apr. 2012) 623–634.
[22] M.R. Prausnitz, R. Langer, Transdermal drug delivery, Nat. Biotechnol. 26 (11) (Nov. 2008) 1261–1268.
[23] C.C. Coussios, R.A. Roy, Applications of acoustics and cavitation to noninvasive therapy and drug delivery, Annu. Rev. Fluid Mech. 40 (1) (Jan. 2008) 395–420.
[24] A. Eller, Rectified diffusion during nonlinear pulsations of cavitation bubbles, J. Acoust. Soc. Am. 37 (3) (1965) 493–503.
[25] B.E. Polat, W.M. Deen, R. Langer, D. Blankschtein, A physical mechanism to explain the delivery of chemical penetration enhancers into skin during transdermal sonophoresis — insight into the observed synergism, J. Control. Release 158 (2) (Mar. 2012) 250–260.
[26] S. Mitragotri, D. Blankschtein, R. Langer, Ultrasound-mediated transdermal protein delivery, Science 269 (5225) (Aug. 1995) 850–853.
[27] S. Danese, C. Fiocchi, Ulcerative colitis, N. Engl. J. Med. 365 (18) (2011) 1713–1725.
[28] E.-J. Park, J. Werner, J. Beebe, S. Chan, N.B. Smith, Noninvasive ultrasonic glucose sensing with large pigs (~200 pounds) using a lightweight cymbal transducer Array and biosensors, J. Diabetes Sci. Technol. 3 (3) (Apr. 2009) 517–523.
[29] C.R. Bawiec, Y. Sunny, A.T. Nguyen, J.A. Samuels, M.S. Weingarten, L.A. Zubkov, P.A. Lewin, Finite element static displacement optimization of 20–100kHz flexural transducers for fully portable ultrasound applicator, Ultrasonics 53 (2) (2013) 511–517.
[30] C.M. Schoellhammer, B.E. Polat, J. Mendenhall, R. Maa, B. Jones, D.P. Hart, R. Langer, D. Blankschtein, Rapid skin permeabilization by the simultaneous application of dual-frequency, high-intensity ultrasound, J. Control. Release 163 (2) (2012) 154–160.
[31] B.E. Polat, J.E. Seto, D. Blankschtein, R. Langer, Application of the aqueous porous pathway model to quantify the effect of sodium lauryl sulfate on ultrasound-induced skin structural perturbation, J. Pharm. Sci. 100 (4) (Apr. 2011) 1387–1397.
[32] T.T. Kararli, Comparison of the gastrointestinal anatomy, physiology, and biochemistry of humans and commonly used laboratory animals, Biopharm. Drug Dispos. 16 (5) (Jul. 1995) 351–380.
[34] M.E. Johansson, H. Sjövall, G.C. Hansson, The gastrointestinal mucus system in health and disease, Nat. Rev. Gastroenterol. Hepatol. 10 (6) (Jun. 2013) 352–361.
[35] S. Hua, E. Marks, J.J. Schneider, S. Keely, Advances in oral nano-delivery systems for colon targeted drug delivery in inflammatory bowel disease: selective targeting to diseased versus healthy tissue, Nanomedicine 11 (5) (Jul. 2015) 1117–1132.
[36] J. Kushner, D. Blankschtein, R. Langer, Evaluation of the porosity, the tortuosity, and the hindrance factor for the transdermal delivery of hydrophilic permeants in the context of the aqueous pore pathway hypothesis using dual-radiolabeled permeability experiments, J. Pharm. Sci. 96 (12) (2007) 3263–3282.
[37] W. Yuan, Y. Lv, M. Zeng, B.M. Fu, Non-invasive measurement of solute permeability in cerebral microvessels of the rat, Microvasc. Res. 77 (2) (Mar. 2009) 166–173.